CALIFORNIA INSTITUTE OF TECHNOLOGY

BIG BEAR SOLAR OBSERVATORY

HALE OBSERVATORIES

SOLAR XUV SPECTRAL IRRADIANCE MONITOR

R.L. Moore

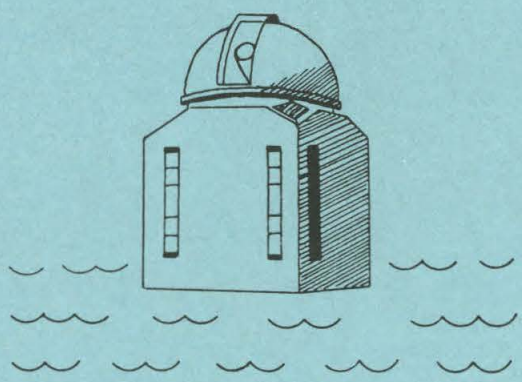

SCIENTIFIC USES, PERFORMANCE REQUIREMENTS AND PRELIMINARY DESIGN CONSIDERATIONS FOR A SOLAR XUV SPECTRAL IRRADIANCE MONITOR

R.L. Moore

BIG BEAR SOLAR OBSERVATORY, HALE OBSERVATORIES
CARNEGIE INSTITUTION OF WASHINGTON
CALIFORNIA INSTITUTE OF TECHNOLOGY

September, 1976
BBSO #0158

ABSTRACT

Scientific uses for an XUV (λ < 3000 Å) spectral flux monitor on the Solar Physics Spacelab and the performance requirements for these uses are defined for the disciplines of solar physics and aeronomy. The study emphasizes solar physics uses with particular emphasis on solar flares. It is concluded that:

1. An XUV monitor which meets the needs of solar physics will also be very useful for aeronomy.
2. The observation of solar flares is the scientific use of greatest potential.
3. The measurement of the XUV flux of a significant number of flares during a Spacelab mission requires a sensitivity of 0.1%.

Some basic design questions posed by the results of the study are briefly discussed.

I. INTRODUCTION

The study reported here was commissioned by the NASA Solar Physics Spacelab Facility Definition Team (FDT) for Quick Response and Special Purpose (QRSP) Experiment Capability. The purpose of the QRSP FDT is to define the scientific objectives, the performance requirements, and the design and operation of the quick response experiments and the special purpose experiments for the Solar Physics Spacelab to be orbited on the NASA Space Shuttle. The Solar Physics Spacelab will consist primarily of facility class instruments for obtaining solar observations of high spatial and spectral resolution in the visible, UV, EUV and X-rays. Special purpose experiments are those experiments for which the facility class instruments will not be well-suited, and which may complement or supplement the observations obtained with the facility class instruments. This report presents a study of the monitoring of the solar XUV spectrum as a potential special purpose experiment for the Solar Physics Spacelab. Here we have followed Goldberg (1967) in taking XUV to designate the entire X-ray and ultraviolet spectrum shortward of 3000 Å, the short wavelength limit for observations from the ground.

The study emphasises the scientific uses of a spectral XUV monitor and the performance requirements necessary for these uses. The design of the monitor is only considered in so far as the basic constraints and alternatives posed

by the scientific uses and performance requirements.

There are two main scientific disciplines for which observations of the solar XUV spectrum are of fundamental importance: solar physics and aeronomy. As solar physics is the primary concern of the Solar Physics Spacelab, the study concentrates on the scientific uses and performance requirements for solar physics. Uses and requirements for aeronomy are also considered, but to a lesser extent and as secondary to solar physics.

The solar physics needs for an XUV monitor are considered for the following topics.

1. Calibration of other Solar Physics Spacelab instruments which observe in the XUV.
2. The non-flaring sun, including the relevance of XUV measurements to possible variations in the solar constant.
3. Solar flares.

Since the Solar Physics Spacelab missions will have durations of only one week to a month, in terms of complementing and supplementing the facility class instruments, it appears that the scientific use of greatest potential for an XUV monitor is the observation of solar flares. Accordingly, the most effort has gone into studying this application. For this purpose, a set of 17 flares which were observed both in X-rays and Hα and analyzed by Moore and Datlowe (1975) are used as the primary data base.

II. SCIENTIFIC USES

A. AERONOMY

1. Stratosphere

Solar radiation from about 2000 Å to 3000 Å is absorbed in the stratosphere (Figure 1) and is responsible for the presence of the stratosphere. It is the absorption of this radiation, mainly by ozone, which causes the temperature increase with height which stabilizes the stratosphere against free convection. Radiation shortward of 2423 Å produces dissociation of diatomic oxygen which results in the formation of ozone.

It is thought that interactions between the stratosphere and the underlying troposphere can affect the weather (Zirin et al., 1976). Present models of the atmosphere indicate that a 10% change in the heating of the stratosphere would produce appreciable changes in the troposphere. Models of the stratosphere and lower ionosphere are sensitive to changes in the 1200-3000 Å solar irradiance of less than 10% (Zirin et al., 1976).

2. Ionosphere

Shortward of about 2000 Å, the solar XUV radiation is absorbed in the ionosphere. Shortward of 1027 Å, the ionization limit for O_2, the radiation is absorbed mainly by ionization. Consequently, the XUV spectrum below 1027 Å

determines the electron content of the ionosphere and its distribution with height.

The XUV radiation from even quite small flares (subflares) produces a sudden increase in the electron content of the ionosphere sufficient to be detected through radio propagation effects such as sudden frequency deviations (Donnelly, 1976). Observations of the radio propagation effects can be combined with models of the ionosphere to estimate the increase in electron content and the corresponding amount of XUV flux (< 1027 Å) produced by the flare. All such estimates of flare XUV flux based on radio measurements of the ionosphere are currently uncertain by at least a factor of four (Donnelly, 1973). About half of the uncertainty is due to lack of knowledge of the shape of the spectrum of the XUV burst, while the other half is due to uncertainties in the ionosphere models. Hence, direct observations of the incident XUV flux to a factor of two or better in a few broad bands spanning the XUV would allow improvements in the ionosphere models and in the calibration of the radio measurements of the electron content changes. This in turn would improve the accuracy of the measurement of the XUV flux from flares by these comparatively inexpensive radio methods.

B. SOLAR PHYSICS

1. Calibration of Other XUV Experiments

Some of the most informative observations of solar

flares from the Skylab missions were soft X-ray filtergrams and EUV spectra-spectroheliograms recorded on photographic film. Presumably similar observations in the XUV will be obtained with the facility class instruments on the Solar Physics Spacelab. Photographs are excellent for recording the spatial structure of flares, but it is difficult to accurately measure absolute intensities especially if the film becomes saturated in some parts of the flare. In this connection it would be very useful to have an independent measure of the total flux from flare in that portion of the spectrum recorded by the photograph. These observations could be obtained with an XUV flux monitor with appropriate spectral selectivity.

For non-flare observations, calibration of the photographic film is less of a problem. Nevertheless, a record of the total output of the sun in the spectral band of interest would be a convenient check on the calibration. Such a record would also provide an independent measure of the integrated effect of large scale features such as coronal holes or extended old plage regions, as well as active regions.

2. Non-Flaring Sun

The solar spectrum shortward of 3000 Å contains radiation emitted from all of the layers or regions of the observable solar atmosphere: photosphere, photosphere-chromosphere temperature minimum, chromosphere, chromosphere-

corona transition, corona and active-region corona. In general, the shorter the wavelength, the greater the temperature and height of the source of emission in the solar atmosphere. For temperatures above 10^4 °K, essentially all of the emission is contained in the XUV spectrum shortward of about 2000 Å. Thus, with sufficient spectral resolution, observations of the XUV spectral irradiance allows the radiative output of the entire solar atmosphere to be measured as a function of temperature above 10^4 °K. Such measurements would provide a basic empirical test for models of the solar atmosphere, both for quiet regions and for active regions.

The degree of constancy of the solar luminosity is of fundamental importance for stellar physics. In addition, climatologists and modelers of the earth's atmosphere estimate that a 0.1% change in the solar constant would produce significant changes in the climate and weather. A change in the solar constant of this magnitude is just at the limit of detectability of present radiometers (Zirin et al., 1976). About 1% of the solar constant is contributed shortward of 3000 Å, with only about 0.01% from below 2000 Å (see Table II). Thus, only the 2000-3000 Å range of the XUV can contribute significantly to measurable changes in the total solar constant. However, it would still be important to compare variations in the observed flux shortward of 2000 Å with any observed changes in the solar constant, as this could give clues as to the physical cause of the change.

3. Flares

a. Total energy

A quantity fundamental to the understanding of any physical phenomenon is the total energy involved in the phenomenon. In solar flares, all of the energy which is not carried away by mass motions, such as ejections or blast waves, must eventually be radiated away. It appears likely that less than half of this contained energy is radiated in the visible (McIntosh and Donnelly, 1972; Zirin and Tanaka, 1973). Therefore, it is essential to measure the total XUV flare output in order to measure the total energy of a flare.

b. Thermal component

Spectral observations of soft ($\lambda > 1$ Å) X-rays from flares show that flares generate thermal plasmas with temperatures of the order of 10^7 °K. The thermal energy content at any instant is given by

$$Q_{th} = 3kTn_eV \ , \qquad (1)$$

where V is the volume of the thermal X-ray plasma. The shape and magnitude of the thermal X-ray spectrum respectively determine the temperature T and the emission measure $H \equiv n_e{}^2V$ of the thermal X-ray plasma. Hence, for given observed values of T and H, the thermal energy content is inversely proportional to the electron number density n_e:

$$Q_{th} = 3kT \frac{H}{n_e} \ . \qquad (2)$$

The electron number density is uncertain by about a factor of ten; it may be anywhere from a few times 10^{10} cm^{-3} to a few times 10^{11} cm^{-3} (Hudson and Ohki, 1972; Widing and Cheng, 1974; Moore and Datlowe, 1975). Consequently, it is necessary to measure the total XUV output of the thermal flare in order to determine the total thermal energy to better than a factor of ten.

Soft X-ray filtergrams of flares show that the thermal X-ray plasma is contained in closed magnetic field arches (Svestka, 1976). This indicates that the thermal X-ray plasma cools primarily by radiation and heat conduction rather than by expansion. The temperature decay time

$$\tau_T \equiv T \left(\frac{dT}{dt} \right)^{-1} \tag{3}$$

for conduction cooling is given approximately by

$$(\tau_T)_c = 3k \frac{L^2 n_e}{\kappa(T)} \quad , \tag{4}$$

and the corresponding radiative cooling time is

$$(\tau_T)_r = 3k \frac{T}{\Lambda_r(T) n_e} \tag{5}$$

(Moore and Datlowe, 1975). Here $\Lambda_r(T)$ is the radiative cooling coefficient which has been computed by Tucker and Koren (1974) (Figure 2), L is the overall length scale of the flare, and $\kappa(T)$ is the thermal conductivity which is given to a good approximation by

$$\kappa = \kappa_c T^{5/2} \quad , \tag{6}$$

$$\kappa_c = 1.0 \times 10^{-6} \text{ erg sec}^{-1} \text{ }^{\circ}\text{K}^{-7/2} \text{ cm}^{-1} .$$

The ratio of the rate of radiative cooling to the rate of conduction cooling is the ratio of the conduction cooling time to the radiative cooling time,

$$\frac{(\tau_T)_c}{(\tau_T)_r} = \frac{\Lambda_r(T)}{\kappa_c T^{7/2}} L^2 n_e^2 . \qquad (7)$$

Due to the factor of ten uncertainty in n_e, the relative importance of conduction cooling and radiative cooling is uncertain by a factor of a hundred. For the 17 flares studied by Moore and Datlowe (1975), Table I gives the minimum, median, and maximum values of log $\{(\tau_T)_c/(\tau_T)_r\}$ at thermal X-ray maximum for $n_e = 10^{10.5}$ cm^{-3} and for $n_e = 10^{11.5}$ cm^{-3}. Table I shows that while for some flares it seems fairly certain that conduction cooling dominates radiative cooling, for many flares it is completely uncertain whether one or the other dominates or whether both processes contribute about equally to the cooling of the thermal X-ray flare plasma.

Observation of the XUV spectrum of the thermal flare could very simply determine the relative importance of conduction cooling and radiative cooling of the thermal X-ray plasma. The calculations of Tucker and Koren (1971) show that at temperatures in the vicinity of 10^7 °K and above, for a plasma of coronal composition, more than 80% of the emitted radiation is at wavelengths shortward of

25 Å (Figure 3). Therefore, observation of much less energy in the XUV spectrum longward of 25 Å than shortward would show that radiative cooling dominates. On the other hand, if the energy radiated from the thermal flare at wavelengths longward of 25 Å (from plasmas at temperatures below 10^7 °K) is supplied primarily by heat conduction from the 10^7 °K thermal X-ray plasma, as is quite plausible, then observation of much more XUV flux longward of 25 Å than shortward would mean that conduction cooling dominates. In general, the ratio of the XUV flux shortward of 25 Å to that longward of 25 Å would be approximately equal to the ratio of the radiative cooling to the conduction cooling, i.e. $(\tau_T)_c/(\tau_T)_r$. Therefore, observation of the XUV spectrum of the thermal flare could establish the ratio of radiative cooling to conduction cooling, and along with measurements of the temperature of the thermal X-ray plasma and of the length scale of the flare, would give an estimate of the number density of the thermal X-ray plasma (from equation (7)).

Another unresolved question regarding the thermal flare is whether (1) there is still substantial heating taking place at thermal X-ray maximum, or (2) essentially all of the thermal energy is generated during the impulsive rise phase of the flare. Observation of the XUV spectrum of the thermal flare could also resolve this question. Once n_e were evaluated by the above procedure, a predicted cooling time given by

$$\frac{1}{(\tau_T)_{pred}} = \frac{1}{(\tau_T)_c} + \frac{1}{(\tau_T)_r} \qquad (8)$$

could be evaluated and compared with the observed cooling time,

$$(\tau_T)_{obs} \equiv \left[T \left(\frac{dT}{dt}\right)^{-1} \right]_{observed} . \qquad (9)$$

Values of $(\tau_T)_{pred}$ much less than $(\tau_T)_{obs}$ would indicate that substantial heating was still in progress, whereas values of $(\tau_T)_{pred}$ approximately equal to $(\tau_T)_{obs}$ would indicate that heating had essentially ended. Values of $(\tau_T)_{pred}$ much greater than $(\tau_T)_{obs}$ would indicate substantial cooling by some process (e.g. expansion) in addition to conduction and radiation.

c. Impulsive component

The rapid rise of the soft X-ray thermal component during the early part of the flare is often accompanied by an impulsive burst of hard ($\lambda < 1$ Å) X-rays. Estimates of the energy content of the high-energy ($\gtrsim 10$ keV) electrons which produce the hard X-rays indicate that these electrons contain as much energy as the thermal plasma at thermal X-ray maximum (Lin and Hudson, 1971, 1976). This suggests that the impulsive hard electrons may be the energy source for the thermal flare. On the other hand, estimates of the total XUV flux from observations of the ionosphere indicate that

the XUV emission during the impulsive phase is about equal to the energy content of the hard electrons (Kane and Donnelly, 1971). This suggests that most of the energy of the hard electrons may be immediately radiated away rather than going into the thermal X-ray plasma. The ionosphere observations determine the XUV flux of the impulsive component to within only about a factor of four at best. Accuracy of better than a factor of two is necessary to resolve the question of whether most of the energy of the impulsive hard electrons is immediately radiated away. XUV observations of comparable accuracy are required for the thermal phase in order to determine the amount of thermal energy for comparison with the energy available from the hard electrons.

III. PERFORMANCE REQUIREMENTS

A. NON-FLARING SUN

1. XUV Spectrum for Medium Activity

A representative solar spectrum from soft X-rays to the near infra-red is given in Figure 4. The XUV portion of the spectrum shortward of 1220 Å was compiled from observations taken during medium levels of activity. The 10.7 cm radio flux level on the various days of observation ranged from about 120 to 190 in units of 10^{-22} $Wm^{-2}Hz^{-1}$. 10.7 cm flux levels of 90 and 220 are respectively typical during

solar minimum and solar maximum (Timothy, 1976). Longward of 20 Å, the spectrum was compiled from the following sources: >1220 Å, Allen (1973); 1220-130 Å, Heroux et al. (1974); 130-52 Å, Malinovsky and Heroux (1973) as corrected by Heroux et al. (1974); 52-20 Å, Freeman and Jones (1970). Shortward of 20 Å, the spectrum was obtained as follows. The 17 flares of Moore and Datlowe (1975) occurred during the period from the beginning of October, 1971 to the end of May, 1972, which was a period of medium activity. The flux level given for the 1.9 to 2.5 Å interval is the median of the non-flare background flux observed by the UCSD OSO-7 experiment near the times of the 17 flares. The 3-8 Å and 8-20 Å flux levels are the medians of the non-flare background fluxes observed by SOLRAD-9 for the same 17 flares and reported in Solar-Geophysical Data.

The variability of the non-flare XUV flux is greater the shorter the wavelength. For the 17 flares used to estimate the XUV spectrum shortward of 20 Å, the ratio between the maximum and minimum background flux was 8 for the 1.9-2.5 Å band, 6 for 3-8 Å, and 6 for 8-20 Å. The flux in the 3-8 Å band may vary by a factor of 20 with variations in the level of activity during solar maximum; the variation over the entire solar cycle is about a factor of 500 (Goldberg, 1967; Kreplin et al., 1976). The variation over the solar cycle decreases with increasing wavelength to about a factor of 100 for 10-20 Å, to less than a factor of 10 for 44-60 Å (Goldberg, 1967), to less than a factor of 2

for the total flux in the 300-1200 Å range (Timothy, 1976). The flux in the interval 1750-2050 Å may vary by 5% to 10% over the solar cycle (Brueckner et al., 1975). Variations of 25% in Lyα 1216 Å, 5% at 1750 Å and 1% at 2950 Å were observed over a solar rotation during the last solar maximum (Heath and Wilcox, 1974).

The total flux in the XUV spectrum in Figure 4 is given in Table II for a division of the spectrum into six wavelength intervals. The ratio of the flux in each interval to the solar constant (1.36×10^6 erg cm^{-2} sec^{-1}) is also given. Less than 0.001% of the solar constant is contributed by radiation shortward of 1600 Å.

Longward of 1600 Å, the solar UV is almost all continuum radiation from the photosphere, whereas shortward of 1600 Å, the XUV spectrum consists almost entirely of emission lines and recombination continua. The two strongest emission lines, Lyα and He II 304 Å, are so strong that they show up as individual spikes in Figure 4. (The values of the flux density in Figure 4 at Lyα and He II 304 Å were obtained by taking the flux in each of these lines to be distributed over an interval of 10 Å.) Lyα contributes about half of the flux in the 1200-1600 Å interval, and has more flux than the entire XUV spectrum shortward of Lyα. He II 304 Å has only about a tenth of the flux in Lyα, but is about five times stronger than any other XUV line. The flux in He II 304 Å is about equal to the flux in the interval 170-220 Å from Fe X-XIV.

2. Spectral Intervals and Selectivity of Temperature Ranges

The six wavelength intervals in Table II were chosen for their good degree of selectivity for the characteristic layers and temperature ranges of the non-flaring solar atmosphere. The temperature distribution of the continuum radiation in the 1200-3000 Å range was obtained from Goldberg(1967). Temperatures were assigned to emission lines and recombination continua as follows. In the references for Figure 4, most of the significantly strong emission lines and continua are identified as to the element and stage of ionization of the emitting atom. Almost all of the emission comes from H, neutral He and various stages of ionization of He, C, N, O, Ne, Mg, Si, S, Ca and Fe. From the results of Cox and Tucker (1969), hydrogen lines were assumed to be emitted mostly at temperatures below 3×10^4 °K, and H Ly continuum and He I lines and continua were assumed to be emitted below 10^5 °K. Lines from an ionized species were assigned the temperature of maximum population for the particular element and stage of ionization. Allen and Dupree (1969) and Cox and Tucker (1969) have computed these temperatures for the relevant stages of ionization for the above elements. The resulting estimated temperature distribution for each wavelength range is given in Table III. The value of most entries is uncertain by about $\pm$ 0.05.

The radiation in the range 2000-3000 Å is emitted entirely from the photosphere, mostly from between 5000 to

6000 °K. Most of the radiation in the 1600-2000 Å interval is continuum emission from near the temperature minimum, and hence is emitted at temperatures below 5000 °K. Emission lines begin to appear shortward of 2000 Å, but they contribute no more than 10% of the flux between 1600 and 2000 Å, and are all emitted at temperatures below 10^5 °K. In the 1200-1600 Å interval about half the flux is from Lyα, a quarter is from other emission lines, and the remaining quarter is continuum from the chromosphere down to the temperature minimum. Lyα and about half of the other line emission comes from temperatures below about 3×10^4 °K, and the rest of the emission lines are from temperatures below 10^5 °K. Thus, about 90% of the emission in the 1600-2000 Å band comes from temperatures above the temperature minimum and below 3×10^4 °K, which corresponds roughly to the chromosphere. In the 300-1200 Å interval 85% of the emission is from the chromosphere-corona transition region between 3×10^4 °K and 10^6 °K, 5% from hydrogen lines below 3×10^4 °K, and about 10% from coronal lines above 10^6 °K. 75% of the emission from 20-300 Å is from coronal temperatures, $1\text{-}3 \times 10^6$ °K, and about 90% of the emission from 1-20 Å is from active-region corona at temperatures above 3×10^6 °K.

The correspondence between the chosen wavelength intervals and the characteristic layers and temperature ranges in the solar atmosphere is recapitulated in Figure 5. In summary, 75% or more of the flux from each of these wavelength intervals is emitted from the corresponding layer

or region of the atmosphere. From the trial of other and more closely spaced wavelength divisions, it appears that significantly improved temperature resolution will result only by resolving individual lines. This would require a spectral resolution of the order of 2 to 5 Å (Timothy, 1976).

3. Accuracy and Stability Requirements

Only the 2000-3000 Å interval is significant for absolute measurements of the solar constant. Since present radiometers have an absolute accuracy of no better than 0.25%, and since about 1% of the solar constant is in the 2000-3000 Å interval, it appears that an absolute accuracy of about 10% for this band would be adequate in connection with absolute measurements of the solar constant.

Absolute measurements of the fluxes shortward of 2000 Å are important for determining the energy balance of each layer and the energy exchange between layers. For example, measurement of the radiative output of the corona and transition region is necessary in order to determine the amount of back-radiation heating of the chromosphere. Since no more than about 80% of the radiation from each characteristic layer can be isolated with broad-band measurements, there is little need for absolute accuracies to be better than 10% to 20%. On the other side, in order to help resolve such problems as the relative contribution of collisional excitation and photo-ionization as in the case of He II 304 Å where the two processes appear to be roughly comparable,

absolute accuracies of better than a factor of 2 are required. Measurements of this accuracy are also needed for modeling of the ionosphere (Donnelly, 1973).

The measurements of changes in the flux levels on a time scale of hours to a month (to measure the global effects of active regions, extended old plage and coronal holes) are as important as absolute measurements. The limit of such measurements is set by the stability of the detector. A reasonable performance requirement is that the monitor should be able to easily measure previously observed amounts of variation. From the observed variabilities summarized in the discussion of the XUV spectrum in Figure 4, it would be desireable to be able to detect the following levels of variability: 1-20 Å, 50%; 20-300 Å, 20%; 300-1200 Å, 10%; 1200-1600 Å, 1-5%; 1600-2000 Å, 1%; 2000-3000 Å, <1%. Relative measurements of these accuracies would be useful for improving models of the ionosphere and stratosphere. In particular, the stability requirement of <1% for the 2000-3000 Å range would be more than adequate for detection of the smallest changes (<10%) which can significantly affect current models of the stratosphere, and for detection of a 0.1% change in the solar constant.

B. FLARES

1. Flare Size

The Solar Physics Spacelab will be in orbit for periods

of from one week to a month. Therefore, a reasonable performance requirement for an XUV monitor is that it be sufficiently sensitive to measure the XUV flux of at least a few flares per week.

The UCSD spectral X-ray experiment on OSO-7 operated from October 7, 1971 to May 18, 1973 (a period of medium activity) during which time it observed 590 subflares and small class 1 flares within the analyzable range of the experiment at an average rate of 1.0 per day. The 17 flares of Moore and Datlowe (1975) are a random sample of these flares. We adopt the median of these 17 flares as the upper lower bound on the size of flare which the XUV monitor should be able to measure.

The average value of the Hα area of these 17 flares is 1.0 helocentric square degree {1 sq. deg. = $(1.2 \times 10^4 \text{ km})^2$}. The minimum, median and maximum Hα areas are 0.3, 0.9 and 2.6 sq. deg., respectively. The Hα area size which divides subflares from class 1 flares is 2.1 sq. deg. Frequency of occurrence increases rapidly with decreasing flare size. Hence, the minimum flare which we require the XUV monitor to be able to measure is a larger-than-average subflare.

2. Flare XUV Emission

a. Thermal emission shortward of 20 Å

All of the 17 flares of Moore and Datlowe were observed in the 1.9-2.5 Å band by the UCSD OSO-7 experiment, and 11 of

these were also observed in the 0-3 Å, 1-8 Å and 8-20 Å bands by SOLRAD-9. At the time of the 1.9-2.5 Å flux maximum in these flares, the minimum, median and maximum values of the average flux density (including background) in erg $cm^{-2}sec^{-1}$ $Å^{-1}$ were respectively $10^{-4.6}$, $10^{-4.3}$ and $10^{-3.0}$ for the 1.9-2.5 Å band; $10^{-3.6}$, $10^{-3.1}$ and $10^{-2.4}$ for the 3-8 Å band; $10^{-3.1}$, $10^{-2.9}$ and $10^{-2.3}$ for the 8-20 Å band. These levels of flux density are shown in Figure 6 in comparison with the non-flare XUV spectrum. The 1-8 Å and 8-20 Å bands together contain essentially all of the thermal flare flux shortward of 20 Å. The thermal flare spectrum falls off so steeply below 3 Å that only a negligibly small fraction of the flux shortward of 8 Å is shortward of 3 Å.

The UCSD OSO-7 experiment observed the soft X-ray spectrum shortward of 2.5 Å. These observations show that this part of the XUV flare spectrum is emitted from plasmas with temperatures just above 10^7 °K. For our 17 reference flares, the minimum, median and maximum temperatures observed at thermal X-ray maximum were respectively 1.1×10^7 °K, 1.3×10^7 °K and 1.7×10^7 °K. The results of Tucker and Koren (1971) in Figure 3 show that more than 80% of the emission from the flare plasma observed by the UCSD experiment is emitted shortward of 25 Å. This suggests that the bulk of the flare emission shortward of 20 Å is emitted from the 10^7 °K plasma. However, in addition to this 10^7 °K plasma, a flare also contains plasma distributed over the entire temperature range of the solar atmosphere. In particu-

lar, a flare contains some plasma at temperatures between $10^{6.5}$ and $10^{7.0}$ °K at which more than 40% of the emission is shortward of 25 Å. Thus, it is not clear whether or not the emission shortward of 20 Å is radiated primarily from the same plasma as that which radiates the emission shortward of 2.5 Å. However, we can answer this question by combining the OSO-7 and SOLRAD-9 observations with the computational results of Tucker and Koren (1971).

The radiative cooling coefficients for the 1.5-8 Å and 8-25 Å bands for emission from a thermal coronal plasma are functions of temperature which have been calculated by Tucker and Koren (1971). The ratio of the emission in these two bands is the ratio of these two coefficients which is the function of temperature given in Figure 7. At temperatures in the vicinity of 10^7 °K, the emission in the 1-8 Å band is practically equal to the emission in the 1.5-8 Å band, and the emission in the 8-20 Å band is 90% of the emission in the 8-25 Å band to within a few percent. Thus, from Figure 7 a "predicted" temperature for the thermal X-ray plasma observed by the UCSD OSO-7 experiment can be obtained from the ratio of the 1-8 Å and 8-20 Å fluxes observed by SOLRAD-9. For the 11 flares which were observed both by OSO-7 and SOLRAD-9, the minimum, median and maximum values of $T_{predicted}$ at the time of 1.9-2.5 Å flux maximum are respectively 1.0×10^7 °K, 1.3×10^7 °K and 1.7×10^7 °K, nearly the same as for the "observed" temperatures derived from the OSO-7 observations.

The distribution of the ratio to $T_{predicted}$ to $T_{observed}$ (Figure 8) shows that the temperatures estimated from the 1-8 Å and 8-20 Å observations agree with those determined from the $\lambda < 2.5$ Å observations usually within 15% and always within 45%, and that there is no apparent tendency for $T_{predicted}$ to be either higher or lower than $T_{observed}$. These results indicate that both the $\lambda < 2.5$ Å thermal X-rays and the 2.5-20 Å thermal X-rays are emitted from the same 10^7 °K plasma.

A further check can be made by comparing the flux shortward of 20 Å predicted by the OSO-7 observations with the flux shortward of 20 Å observed by SOLRAD-9. The predicted flux values are obtained from the radiative cooling coefficient curves of Tucker and Koren for the 1.5-8 Å and 8-25 Å bands and the values of temperature and emission measure derived from the OSO-7 observations. The comparison of the predicted and observed fluxes shortward of 20 Å at the time of 1.9-2.5 Å flux maximum in the 11 reference flares is given in Figure 9. For the two weakest flares, the observed flux is larger than the predicted flux by factors of 5 and 3. This may be a real effect, or it may be due only to the difficulty of accurately subtracting the background flux in cases of very weak flares when only the SOLRAD-9 time plots published in Solar-Geophysical Data are used, as was done here. In any case, for all of the stronger flares the predicted and observed fluxes differ by less than 70% with no apparent bias for the observed fluxes to be larger or smaller than predicted. This

indicates that for flares of median size and larger, in which we are primarily interested here, the soft X-rays shortward of 20 Å are emitted predominantly by the $T \gtrsim 10^7$ °K plasma in the thermal flare.

We therefore have the following two results for the thermal flare XUV spectrum.

1. The 1-20 Å band isolates about 80% of the emission from the $T \gtrsim 10^7$ °K thermal flare plasma.
2. The division of the 1-20 Å band into just two bands, such as 1-8 Å and 8-20 Å, is sufficient to adequately determine the temperature and emission measure of the $T \gtrsim 10^7$ °K plasma.

b. Empirical model XUV spectra for subflares

Except for ionospheric measurements, which have essentially no spectral resolution, spectral observations covering a large fraction of the XUV spectrum have been obtained for very few flares. Donnelly (1976) has constructed an empirical model XUV spectrum shortward of 1027 Å for the thermal component of a subflare by combining observations of several different flares. The basic data consist of soft X-ray observations of subflares plus scaled fluxes from ionospheric and OSO-5 XUV observations of the thermal component of two class 2 flares. This spectrum is shown in Figure 10 in comparison with the non-flare spectrum. Here the 8-20 Å flux was set at 10^{-2} erg cm^{-2} sec^{-1}, which is the median value for our 11 reference flares at thermal X-ray maximum.

In this model spectrum, the 8-20 Å band contains only 10% of the total flux shortward of 1027 Å, so that there is about 8 times more flux longward of 20 Å than shortward. This would indicate that conduction cooling of the 10^7 °K plasma dominates radiative cooling. However, just how typical this spectrum is for actual subflares is, of course, highly uncertain.

Figure 11 gives an empirical model XUV spectrum for the impulsive component of a subflare. This spectrum was also constructed by Donnelly (1976) from combined satellite and ionospheric XUV observations of a class 1 flare. We have scaled the spectrum so that the total flux is 0.1 erg cm^{-2} sec^{-1}, the total flux of the spectrum in Figure 10. The ratio of the maximum XUV fluxes in the impulsive and thermal components is typically of the order of unity (Donnelly, 1976). The basic and most firmly established difference between the impulsive component spectra and the thermal component spectra is that the impulsive spectra are flatter, so that there is a much smaller fraction of the total flux shortward of about 100 Å.

3. Accuracy and Sensitivity Requirements

Absolute accuracy requirements for the measurements of flare XUV fluxes are similar to those for observations of the non-flaring solar atmosphere. The basic aim is to be able to estimate the energy balance of the flare plasma in each of the characteristic temperature ranges and to estimate amounts

of energy flow from one temperature range to another. For example, we wish to be able to determine the relative amounts of conduction cooling and radiative cooling of the thermal X-ray plasma. This requires absolute accuracies of better than a factor of 2, but due to the limitations on temperature range selectivity by broad-band observations, there is little to be gained from absolute accuracies of better than 10% to 20%.

The sensitivity requirements are relatively more stringent. The model XUV spectra in Figures 10 and 11 indicate that a sensitivity of the order of 1% is required for measurement of XUV fluxes longward of 20 Å in our median subflare. However, the reliability of these model spectra is very uncertain.

From the standpoint of understanding energy processes in flares, a reasonable sensitivity requirement is that fluxes comparable to those measured in the 1-20 Å band in the thermal flare should be measurable in each of the other wavelength bands in Figure 5. The median energy flux shortward of 20 Å in the 11 reference flares at thermal X-ray maximum is 1.4×10^{-2} erg cm^{-2} sec^{-1}. The ratio of this flux to the background flux in each of the six wavelength intervals is given in Table IV. Table IV shows that a sensitivity of 0.1% would allow accurate measurement of this amount of flux down to 1200 Å and detectability of this flux in the 1200-1600 Å band from the chromosphere. Although the 1600-2000 Å and 2000-3000 Å photospheric bands would be inaccessable, 0.1%

sensitivity would probably allow more than half of the total radiative output of the flare to be measured. Thus, 0.1% seems to be a reasonable minimum requirement for the sensitivity of the XUV monitor longward of 20 Å.

4. Time Resolution

The UCSD solar X-ray experiment on OSO-7 demonstrated that 10 sec time resolution is adequate for observing the development of soft X-rays in subflares. On the other hand, since the impulsive hard X-ray burst in subflares often lasts for only several 10's of seconds, the time resolution of the XUV monitor should not be much worse than about 10 sec in order to resolve the simultaneous impulsive XUV burst.

C. SUMMARY OF PERFORMANCE REQUIREMENTS

The performance requirements considered in the preceding subsections A and B are summarized in Table V. For the most part, these are minimum requirements for the acquisition of data of value for each scientific use. The sources from which most of these requirements were obtained are as follows: Aeronomy: Zirin et al. (1976), Donnelly (1973); Solar Constant: Zirin et al. (1976); Solar Atmosphere: Goldberg (1967), Kreplin et al. (1976), Timothy (1976), Heath and Wilcox (1974); Flares: this study.

Table V shows that an XUV monitor which meets the performance requirements for studies of the solar atmosphere

and solar flares will also meet or surpass the minimum requirements for aeronomy and the solar constant, except for absolute accuracy in the 1200-3000 Å range. Table V also shows that the requirements for the non-flaring solar atmosphere and for flares are for the most part incompatible. Solar atmosphere uses require much higher stability, whereas flares require much higher sensitivity and time resolution.

IV. DESIGN CONSIDERATIONS

A. NON-FLARE MONITORING

Perhaps the first question to be answered preliminary to the design of an XUV monitor for Solar Physics Spacelab is whether or not the non-flare XUV flux will be adequately measured by other monitors which will be in orbit during the early 1980's. SOLRAD-11 is now in orbit and monitors much of the XUV spectrum. The accuracy, stability, sensitivity and expected lifetime of these experiments were not available at the time of this study (Kreplin, private communication). The performance capabilities of these and any other planned XUV monitors should be determined as a first step in any design study for an XUV monitor for Spacelab.

B. FLARE MONITORING

It seems unlikely that any currently operating or designed XUV monitor meets the sensitivity requirement of

0.1% of the total background flux shortward of 1600 Å found in this study for observing subflares. The basic design question here is whether or not this sensitivity can be achieved without imaging. Since the subflares to be observed have linear dimensions of the order of 1 arc min, spatial resolution of 1 arc min would increase the flare-to-background flux ratio by more than a factor of 100. This would make the 1600-2000 Å temperature-minimum band accessible with 1% sensitivity.

C. COMPATIBILITY WITH THE SMM SATELLITE

It is currently planned that the Space Shuttle will retrieve the Solar Maximum Mission (SMM) satellite for refurbishment and improvement. The XUV flux monitor considered here would provide very useful data even without accompanying observations from the facility class instruments on Solar Physics Spacelab. If the XUV monitor were flown on a refurbished version of the SMM satellite, it would provide long-term coverage of the sun as well as support the Solar Physics Spacelab missions. Therefore, consideration should be given to designing the XUV monitor to be compatible with the SMM satellite.

V. CONCLUSIONS

The more important conclusions reached in this study are the following:

1. The scientific use of the greatest potential for an XUV monitor on the Solar Physics Spacelab is the measurement of the XUV flux from flares.

2. Measurements of the XUV flux from flares are necessary for measurement of the total energy released and for measurement of heating and cooling rates both in the impulsive and thermal components.

3. In order to observe a few flares per week, the XUV monitor must be sufficiently sensitive to measure the XUV flux of subflares having Hα areas as small as 1.0 sq. deg. This requires a full-disk flux sensitivity of 0.1% in the 20-1600 Å range.

4. The 1-20 Å band isolates about 80% of the emission from the $T \gtrsim 10^7$ °K thermal X-ray flare plasma.

5. The division of the 1-20 Å band into just two bands, such as 1-8 Å and 8-20 Å, is sufficient to adequately determine the temperature and emission measure of the $T \gtrsim 10^7$ °K flare plasma.

6. The XUV spectrum of the non-flaring sun can be divided into six wavelength intervals in each of which 75% or more

of the flux is emitted from a corresponding characteristic layer and temperature range of the solar atmosphere:

1-20 Å: active-region corona, $> 3 \times 10^6$ °K

20-300 Å: corona, $1\text{-}3 \times 10^6$ °K

300-1200 Å: chromosphere-corona transition region, $3 \times 10^4 - 1 \times 10^6$ °K

1200-1600 Å: chromosphere, $< 5 \times 10^3 - 3 \times 10^4$ °K

1600-2000 Å: temperature minimum, $< 5 \times 10^3$ °K

2000-3000 Å: photosphere, $5\text{-}6 \times 10^3$ °K.

ACKNOWLEDGEMENTS

This study was undertaken at the suggestion and encouragement of Loren Acton and Jake Wolfson. Barry LaBonte was particularly helpful in pointing out key observational papers on the solar XUV spectrum. During the course of the study, I benefited from discussions with Dick Blake, Ken Dere, Dick Donnelly, Hugh Hudson, Gordon Hurford, Sharad Kane, Bob Kreplin and Bob Lin.

This research was funded by the National Aeronautics and Space Administration through the Quick Response and Special Purpose Facility Definition Team for the Solar Physics Spacelab.

REFERENCES

Allen, C.W.: 1973, Astrophysical Quantities, Athlone Press, University of London.

Allen, J.W. and Dupree, A.K.: 1969, Astrophys. J. 155, 27.

Brueckner, G.E., Bartoe, J.-D.F., Moe, O.K., and Van Hoosier, M.E.: 1975 in H. Zirin and J. Walter (eds.) Proceedings of the Workshop: The Solar Constant and the Earth's Atmosphere, Big Bear Solar Observatory Report #0149, p. 71.

Cox, D.P. and Tucker, W.H.: 1969, Astrophys. J. 157, 1157.

Donnelly, R.F.: 1973, in R. Ramaty and R.G. Stone (eds.), High Energy Phenomena on the Sun Symp. Proc., Goddard Space Flight Center, p. 242.

Donnelly, R.F.: 1976, preprint, "Empirical Models of Solar Flare X-Ray and EUV Emission for Use in Studying Their E- and F-Region Effects," to appear in J. Geophys. Res.

Freeman, F.F. and Jones, B.B.: 1970, Solar Phys. 15, 288.

Goldberg, L.: 1967, Ann. Rev. Astron. Astrophys. 5, 279.

Heath, D.F. and Wilcox, J.M.: 1974 in W.R. Bandeen and S.P. Maran (eds.), Possible Relationships between Solar Activity and Meterological Phenomena, Goddard Space Flight Center, p. 116.

Heroux, L., Cohen, M., and Higgins, J.E.: 1974, J. Geophys. Res. 79, 5237.

Hudson, H.S. and Ohki, K.: 1972, Solar Phys. 23, 155.

Kane, S.R. and Donnelly, R.F.: 1971, Astrophys. J. 164, 151.

Kreplin, R.W., Dere, K.P., Horan, D.M., and Meekings, J.F.: 1976, preprint to appear in O.R. White, J.A. Eddy and D.F. Heath (eds.), The Physical Output of the Sun and Its Variation.

Lin, R.P. and Hudson, H.S.: 1971, Solar Phys. 17, 412.

Lin, R.P. and Hudson, H.S.: 1976, preprint "Non-Thermal Processes in Large Solar Flares."

Malinovsky, M. and Heroux, L.: 1973, Astrophys. J. 181, 1009.

McIntosh, P.S. and Donnelly, R.F.: 1972, Solar Phys. 23, 444.

Moore, R.L. and Datlowe, D.W.: 1975, Solar Phys. 43, 189.

Timothy, J.G.: 1976, preprint to appear in O.R. White, J.A. Eddy and D.F. Heath (eds.), The Physical Output of the Sun and Its Variation.

Tucker, W.H. and Koren, M.: 1971, Astrophys. J. 168, 283.

Svestka, Z.: 1976, Solar Flares, D. Reidel Publishing Co., p. 113.

Widing, K.G. and Cheng. C.-C.: 1974, Astrophys. J. 194, L111.

Zirin, H., Moore, R.L., and Walter, J. (eds.): 1976, preprint "Proceedings of the Workshop: The Solar Constant and the Earth's Atmosphere," to appear in Solar Phys.

Zirin, H. and Tanaka, K.: 1973, Solar Phys. 32, 173.

FIGURE CAPTIONS

Figure 1. Height of unit optical depth in the earth's atmosphere as a function of wavelength for vertically incident XUV radiation. From Allen (1973).

Figure 2. Temperature dependence of the total radiative cooling coefficient for a thermal plasma of coronal composition. From Tucker and Koren (1971).

Figure 3. Temperature dependence of the percent of the total emission which is emitted shortward of 25 Å from a thermal coronal plasma. From Tucker and Koren (1971).

Figure 4. Representative XUV and visible spectrum for the non-flaring sun.

Figure 5. Correspondence between XUV wavelength ranges and temperature ranges and layers of the solar atmosphere.

Figure 6. Minimum (---), median (——), and maximum (---) flux levels shortward of 20 Å observed for 17 flares by OSO-7 and for 11 of these flares by SOLRAD-9.

Figure 7. Temperature dependence of the ratio of 1.5-8 Å emission to 8-25 Å emission from a thermal coronal plasma. From Tucker and Koren (1971).

Figure 8. Distribution of the ratio of $T_{predicted}$ from SOLRAD-9 observations to $T_{observed}$ from OSO-7 observations for the 11 reference flares.

Figure 9. Comparison of the flux shortward of 20 Å observed by SOLRAD-9 to the flux predicted from the OSO-7 observations for the 11 reference flares.

Figure 10. Empirical model XUV spectrum for the thermal component of the median reference flare. From Donnelly (1976).

Figure 11. Empirical model XUV spectrum for the impulsive component of the median reference flare. From Donnelly (1976).

TABLE I

POSSIBLE RATIOS OF RADIATIVE COOLING TO CONDUCTION COOLING IN THE 17 FLARES OF MOORE and DATLOWE

$\log n_e$ (cm^{-3})	$\log \left[(\tau_T)_c / (\tau_T)_r \right]$		
	min	median	max
10.5	-3.2	-1.5	-0.8
11.5	-2.2	0.5	1.2

TABLE II

ENERGY FLUX IN THE XUV SPECTRUM OF THE NON-FLARING SUN

λ range (Å)	flux at 1AU (erg cm^{-2} sec^{-1})	fraction of solar constant
1 - 20	8.3×10^{-3}	6.1×10^{-9}
20 - 300	1.6	1.2×10^{-6}
300 - 1200	1.6	1.2×10^{-6}
1200 - 1600	9.8	7.2×10^{-6}
1600 - 2000	2.2×10^{2}	1.6×10^{-4}
2000 - 3000	1.6×10^{4}	1.2×10^{-2}
1 - 3000	1.6×10^{4}	1.2×10^{-2}

TABLE III

TEMPERATURE DISTRIBUTION OF THE XUV FLUX
FROM THE NON-FLARING SUN

λ range (Å)	Fraction of flux emitted at or below given temp. log T(°K)						
	4.0	4.5	5.0	5.5	6.0	6.5	7.0
2000 - 3000	1.0						
1600 - 2000	0.9	0.95	1.0				
1200 - 1600	0.25	0.9	1.0				
300 - 1200		0.05	0.75	0.85	0.9	0.95	1.0
20 - 300			0.1	0.1	0.2	0.95	1.0
1 - 20						0.1	1.0

TABLE IV

RATIO OF MEDIAN FLARE 1 - 20 Å FLUX (1.4×10^{-2} erg cm^{-2} sec^{-1}) TO NON-FLARE FLUX

λ range (Å)	$\frac{\text{1 - 20 Å flare flux}}{\text{non-flare flux}}$
1 - 20	1.7
20 - 300	8.8×10^{-3}
300 - 1200	8.8×10^{-3}
1200 - 1600	1.4×10^{-3}
1600 - 2000	6.4×10^{-5}
2000 - 3000	8.8×10^{-7}

TABLE V

PERFORMANCE REQUIREMENTS

Performance Category and Wavelength Interval (Å)	Scientific Use			
	Aeronomy	Solar Physics		
		Solar Const.	Solar Atm.	Flares
Time Resolution				
1 - 1200	10 sec	-	hours	10 sec
1200 - 3000	hours	hours	hours	10 sec
Absolute Accuracy				
1 - 1200	< factor of 2	-	< factor of 2	< factor of 2
1200 - 3000	10%	10%	< factor of 2	< factor of 2
Stability (over 1 month)				
1 - 20	< factor of 2	-	50%	< factor of 2
20 - 300	< factor of 2	-	20%	< factor of 2
300 - 1200	< factor of 2	-	10%	< factor of 2
1200 - 1600	< 10%	-	1 - 5%	< factor of 2
1600 - 2000	< 10%	-	1%	< factor of 2
2000 - 3000	< 10%	10%	< 1%	< factor of 2
Sensitivity				
1 - 20	50%	-	50%	20%
20 - 300	0.5%	-	20%	0.1%
300 - 1200	0.5%	-	10%	0.1%
1200 - 1600	< 10%	-	1 - 5%	0.1%
1600 - 2000	< 10%	-	1%	0.01%
2000 - 3000	< 10%	1%	< 1%	0.0001%

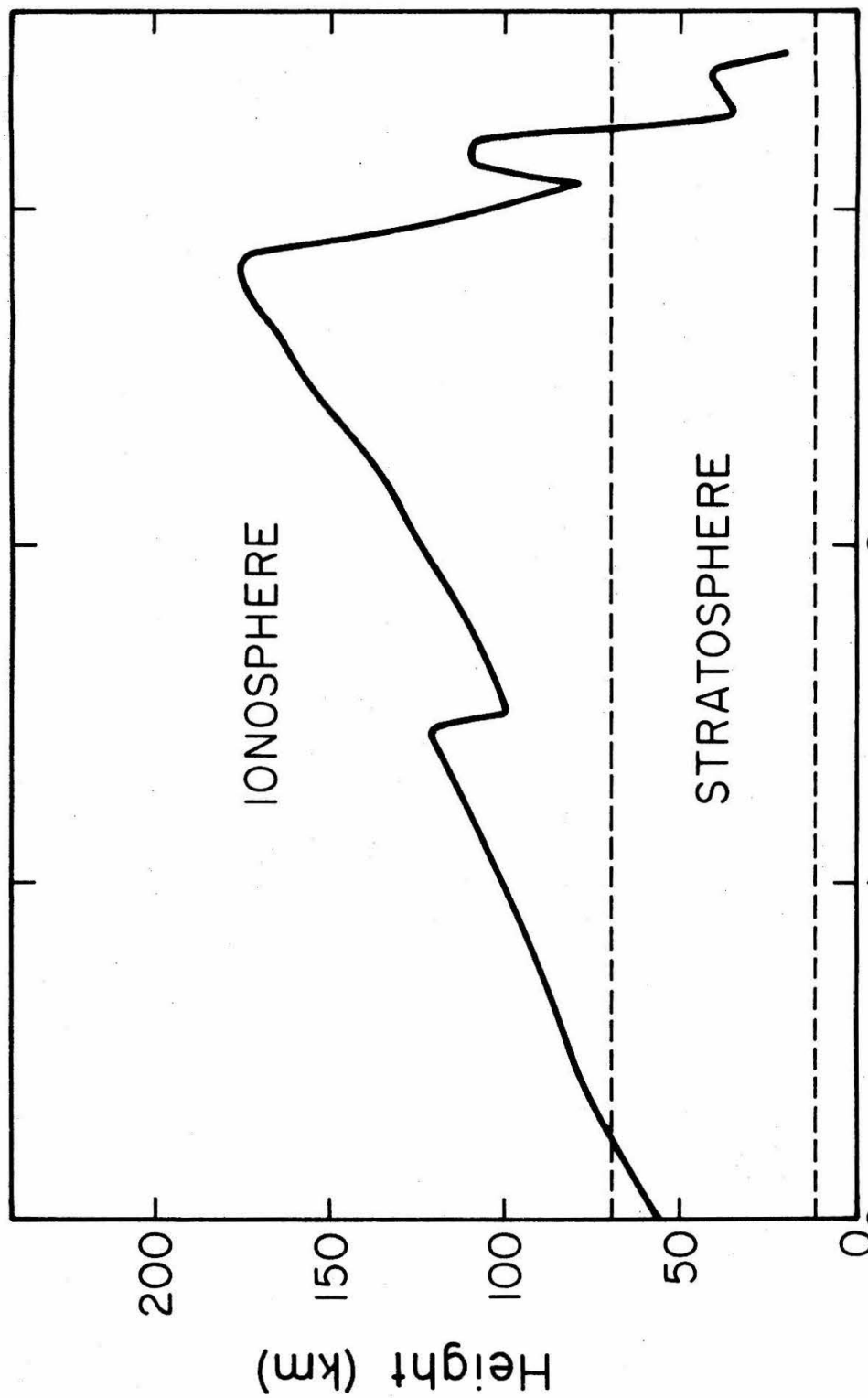
IONOSPHERE
STRATOSPHERE
Height (km)
200
150
100
50
0
0
1
2
3
Log10 λ (Å)

Figure 1

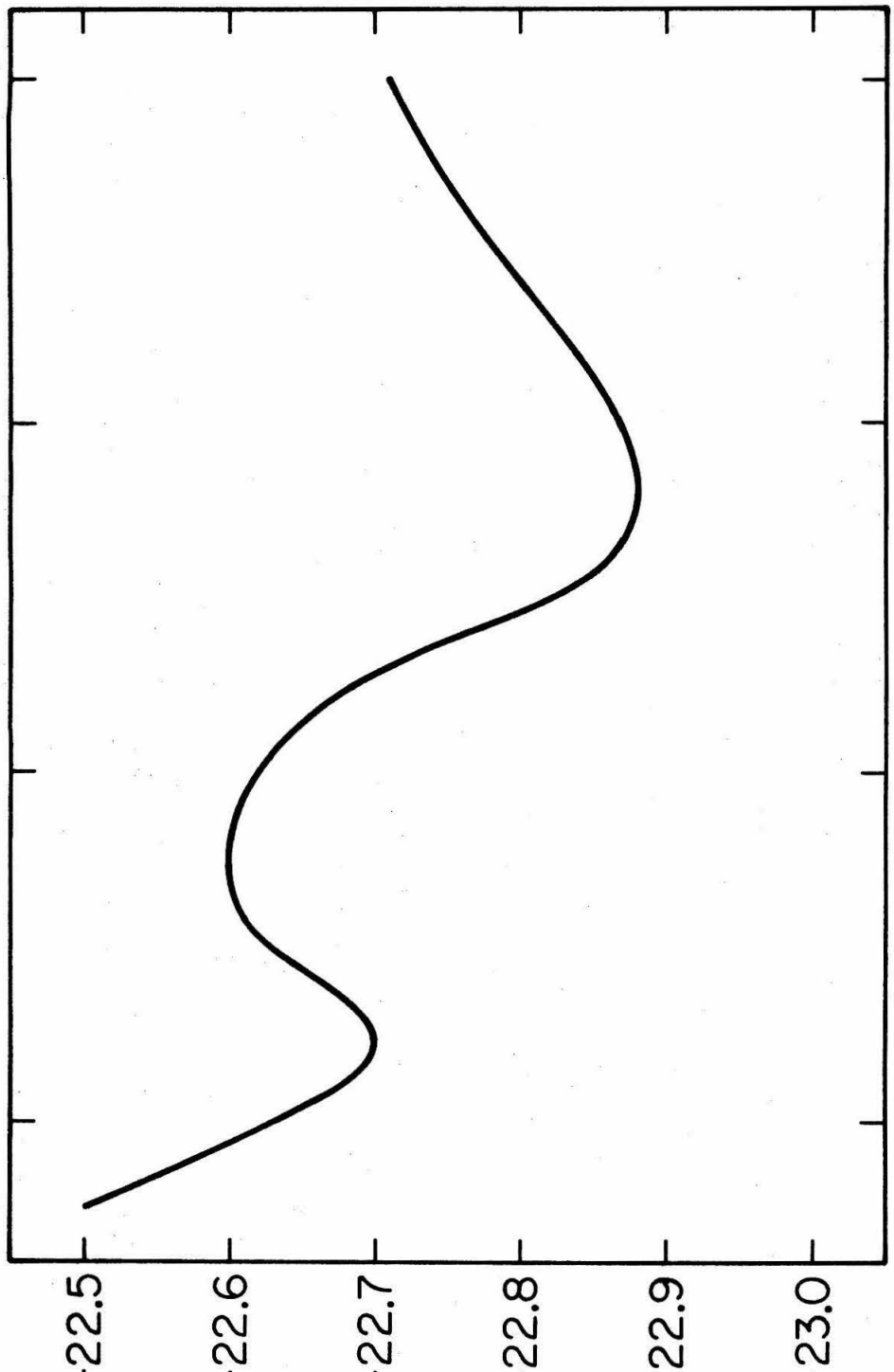
-22.5
-22.6
-22.7
-22.8
-22.9
-23.0
6.5
7.0
7.5
8.0
Log10 T (°K)
Log10 $\frac{n_e n_i P}{}$ (erg cm^3 sec^{-1})

Figure 2

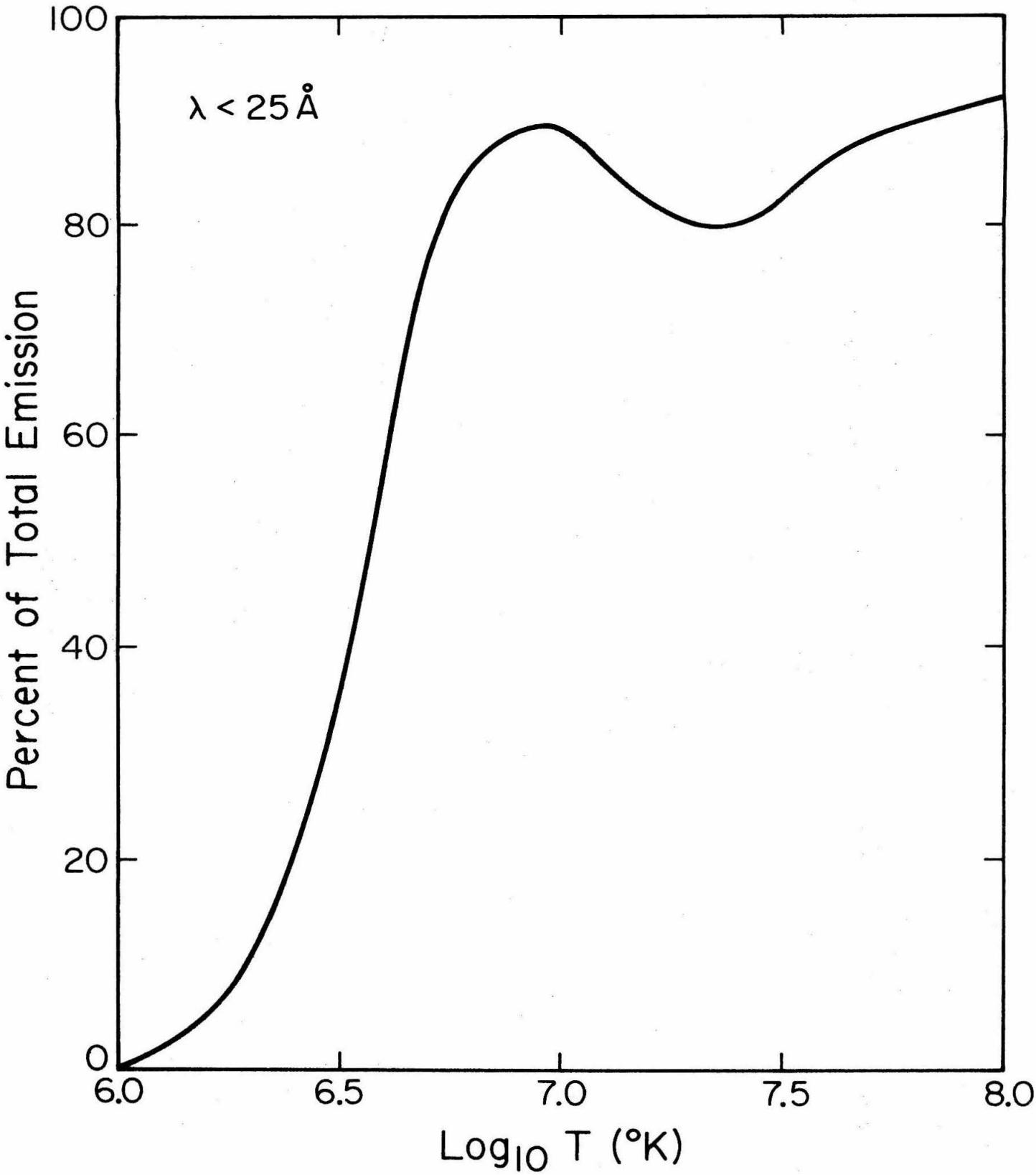
100
λ < 25 Å
80
60
40
20
0
Percent of Total Emission
6.0
6.5
7.0
7.5
8.0
Log10 T (°K)

Figure 3

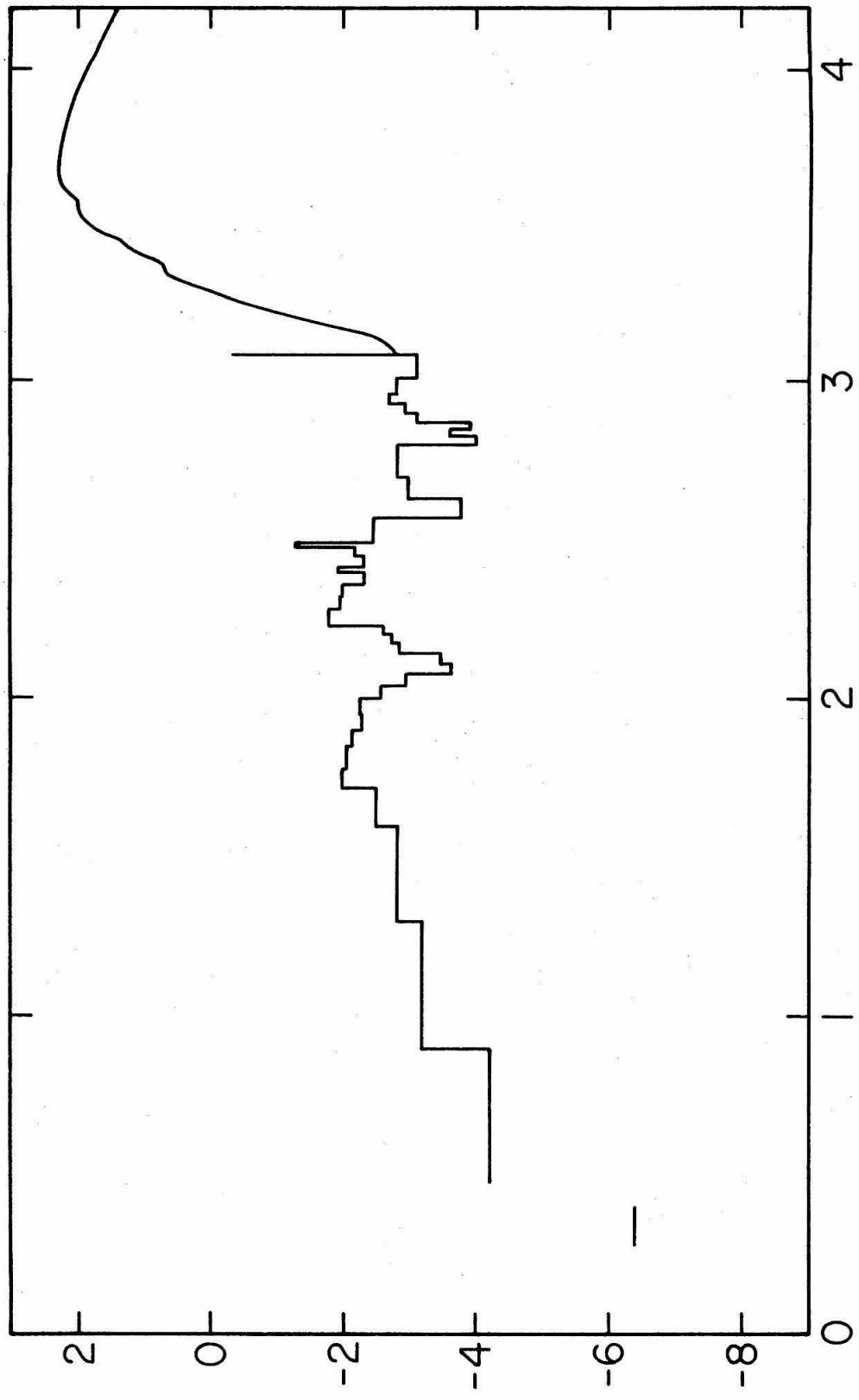

Figure 4

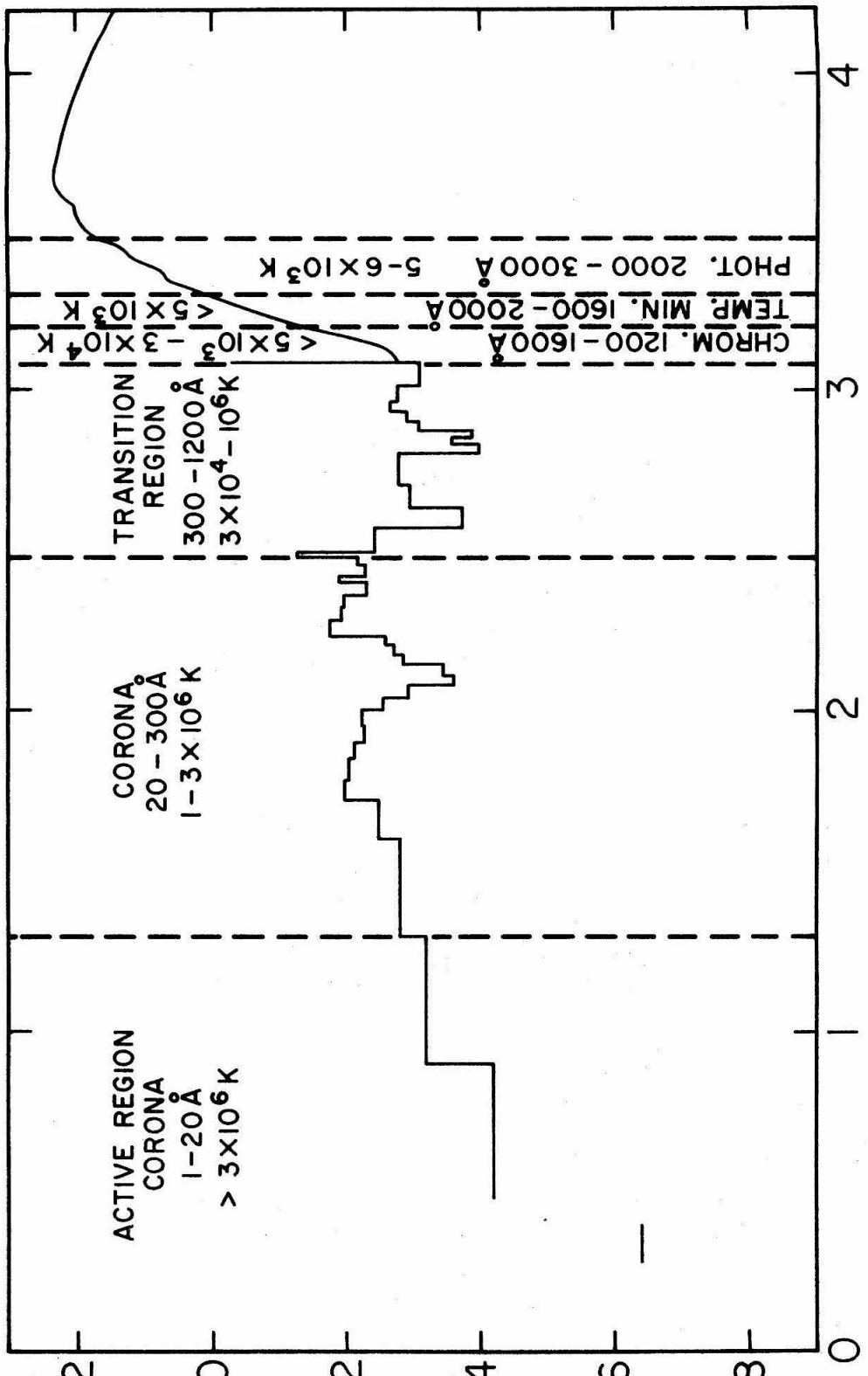
ACTIVE REGION CORONA
1-20Å
> 3X10^6 K
CORONA
20-300Å
1-3X10^6 K
TRANSITION REGION
300-1200Å
3X10^4-10^6K
CHROM. 1200-1600Å
< 5X10^3 - 3X10^4 K
TEMP. MIN. 1600-2000Å
< 5X10^3 K
PHOT. 2000-3000Å
5-6X10^3 K
Log10 fλ (erg cm^-2 s^-1 Å^-1)
Log10 λ(Å)
2
0
-2
-4
-6
-8
0
1
2
3
4

Figure 5

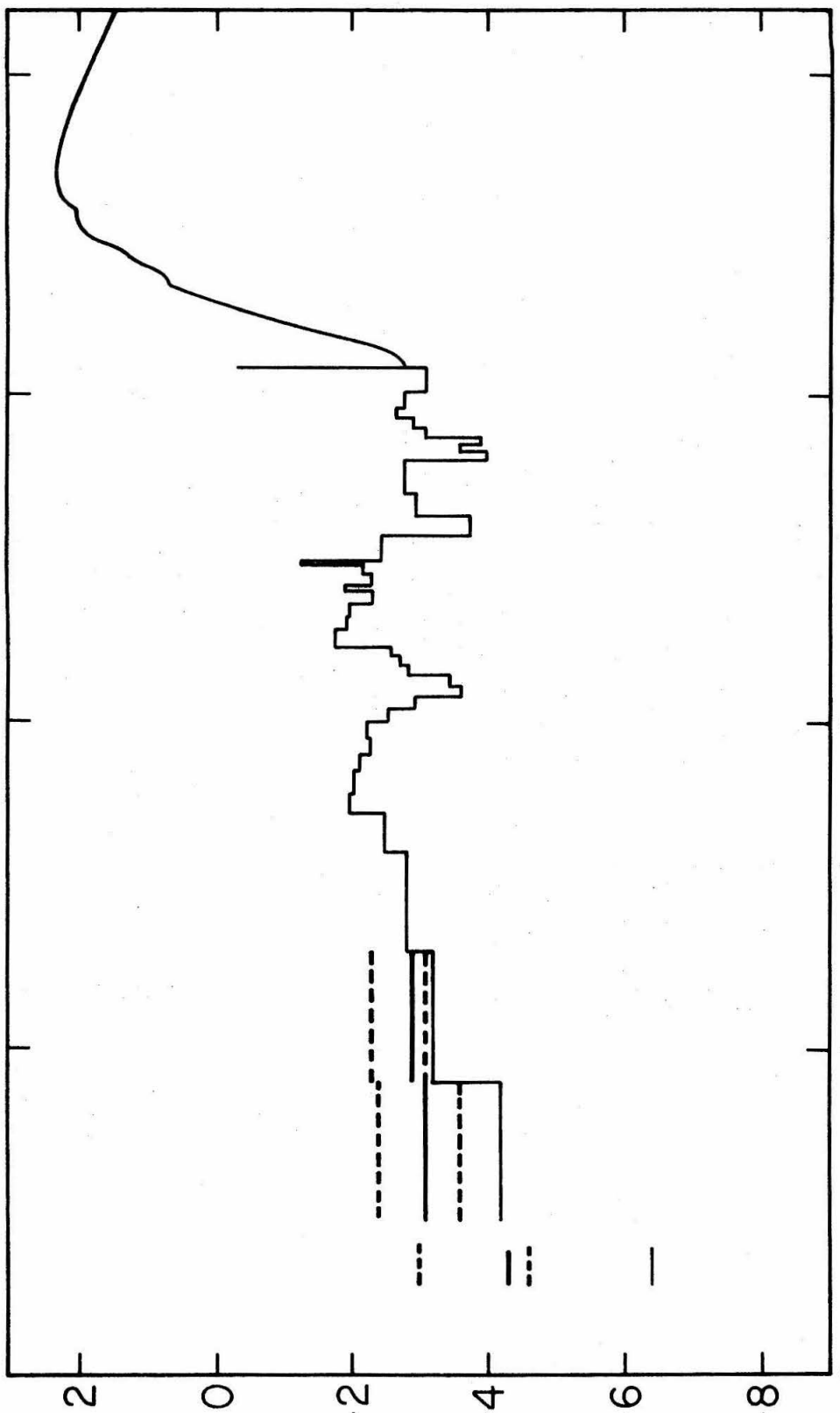

Figure 6

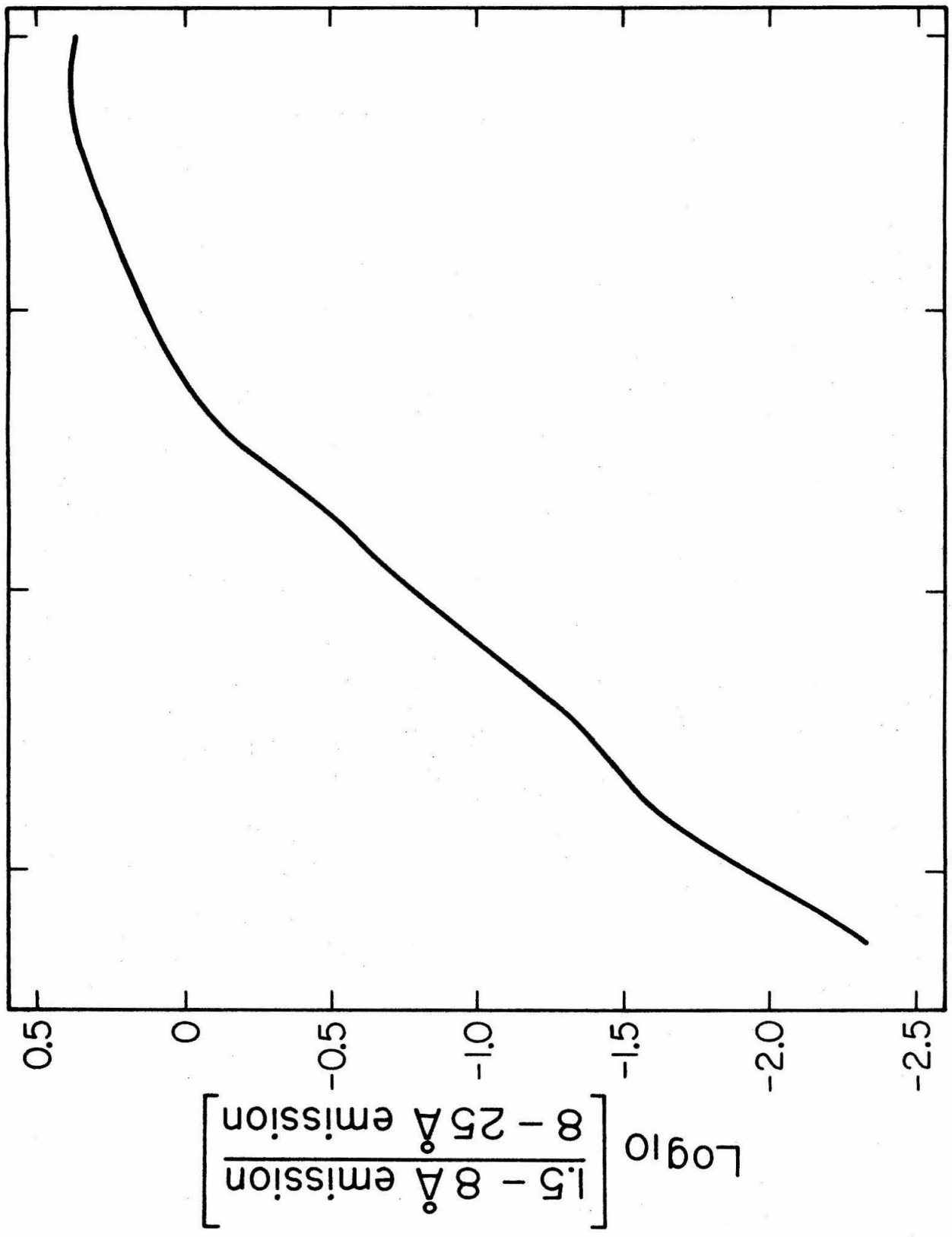
0.5
0
-0.5
-1.0
-1.5
-2.0
-2.5
6.5
7.0
7.5
8.0
Log10 T (°K)
Log10 [1.5 – 8 Å emission / 8 – 25 Å emission]

Figure 7

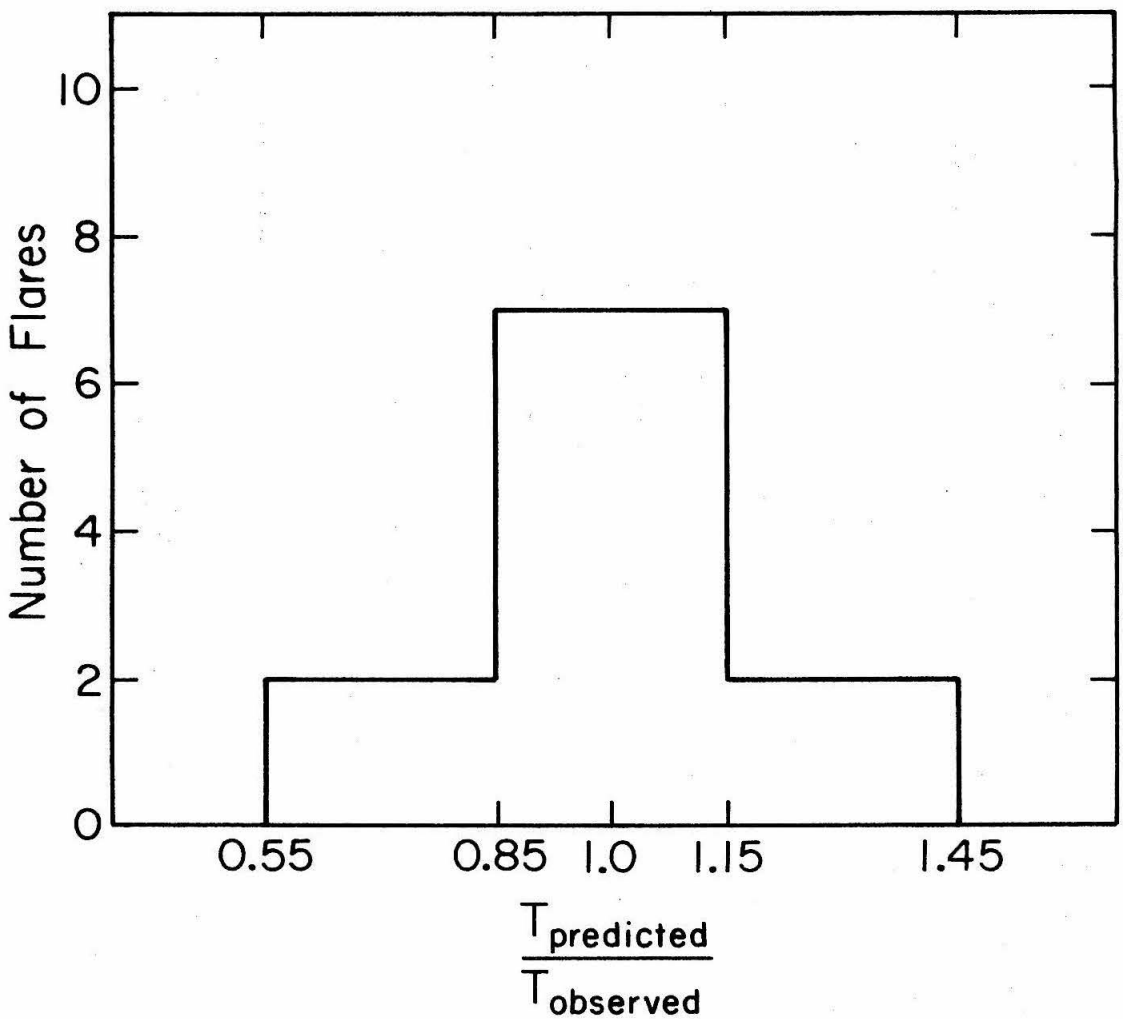
Number of Flares
0
2
4
6
8
10
0.55
0.85
1.0
1.15
1.45
T predicted
T observed

Figure 8

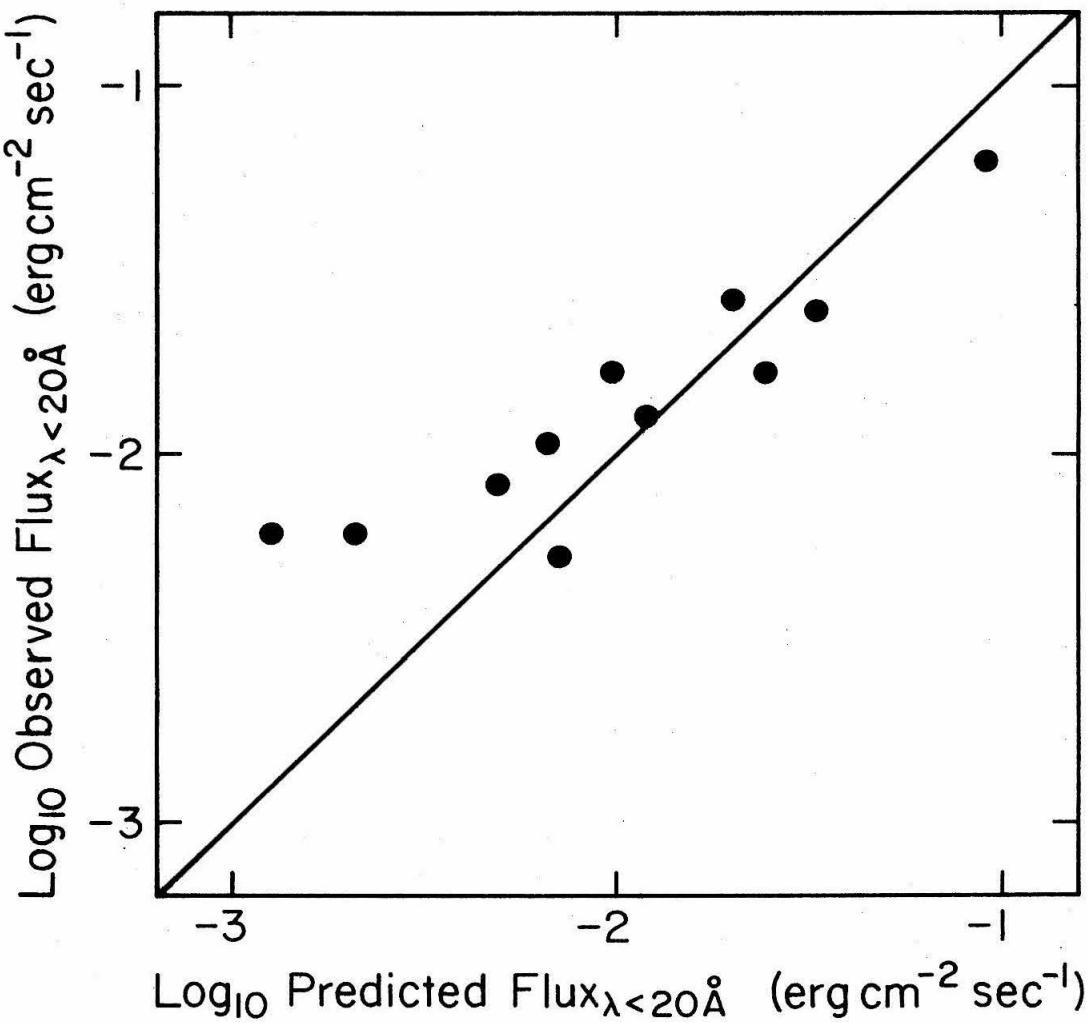
Log10 Observed Flux λ<20Å (erg cm-2 sec-1)
-1
-2
-3
-3
-2
-1
Log10 Predicted Flux λ<20Å (erg cm-2 sec-1)

Figure 9

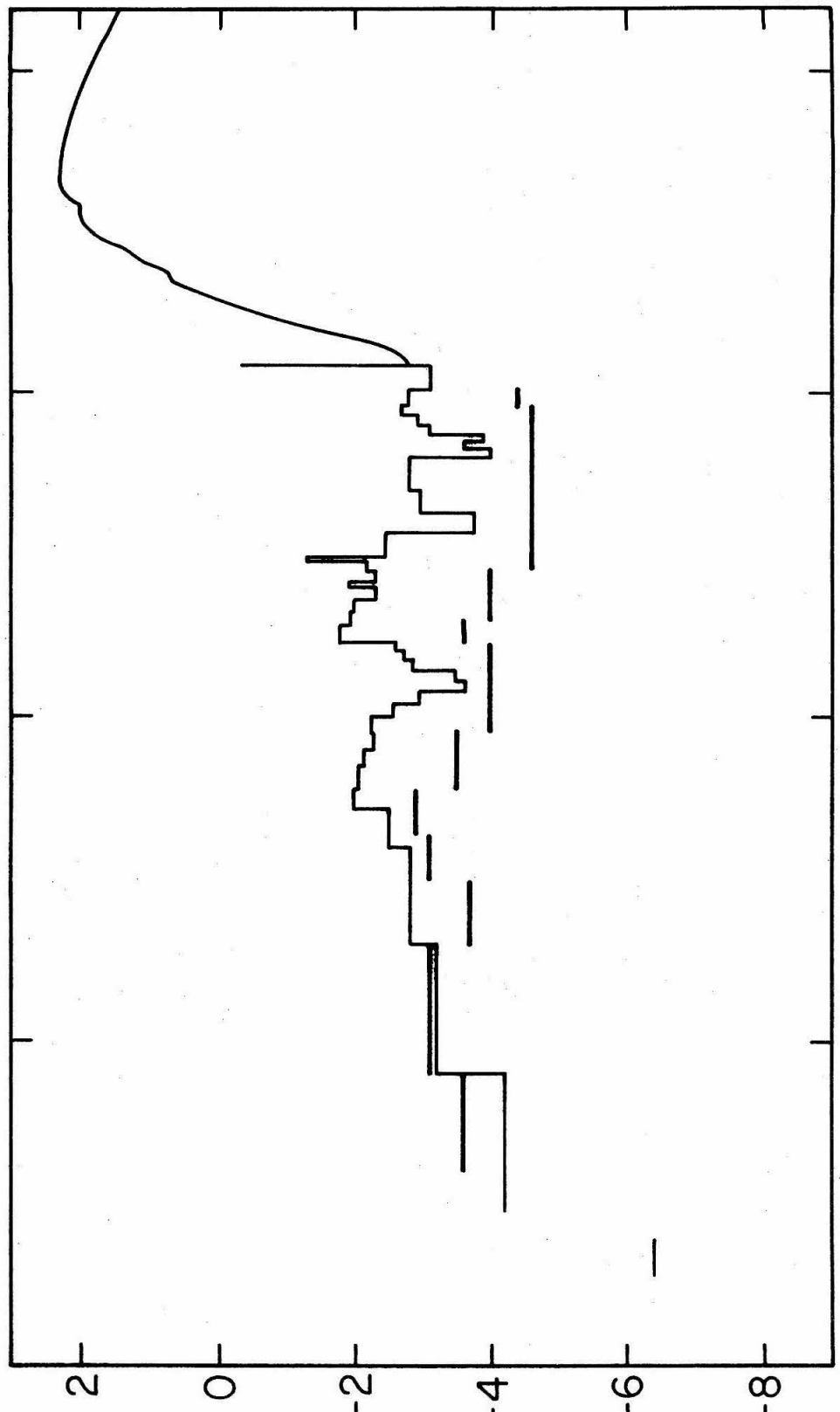

Figure 10

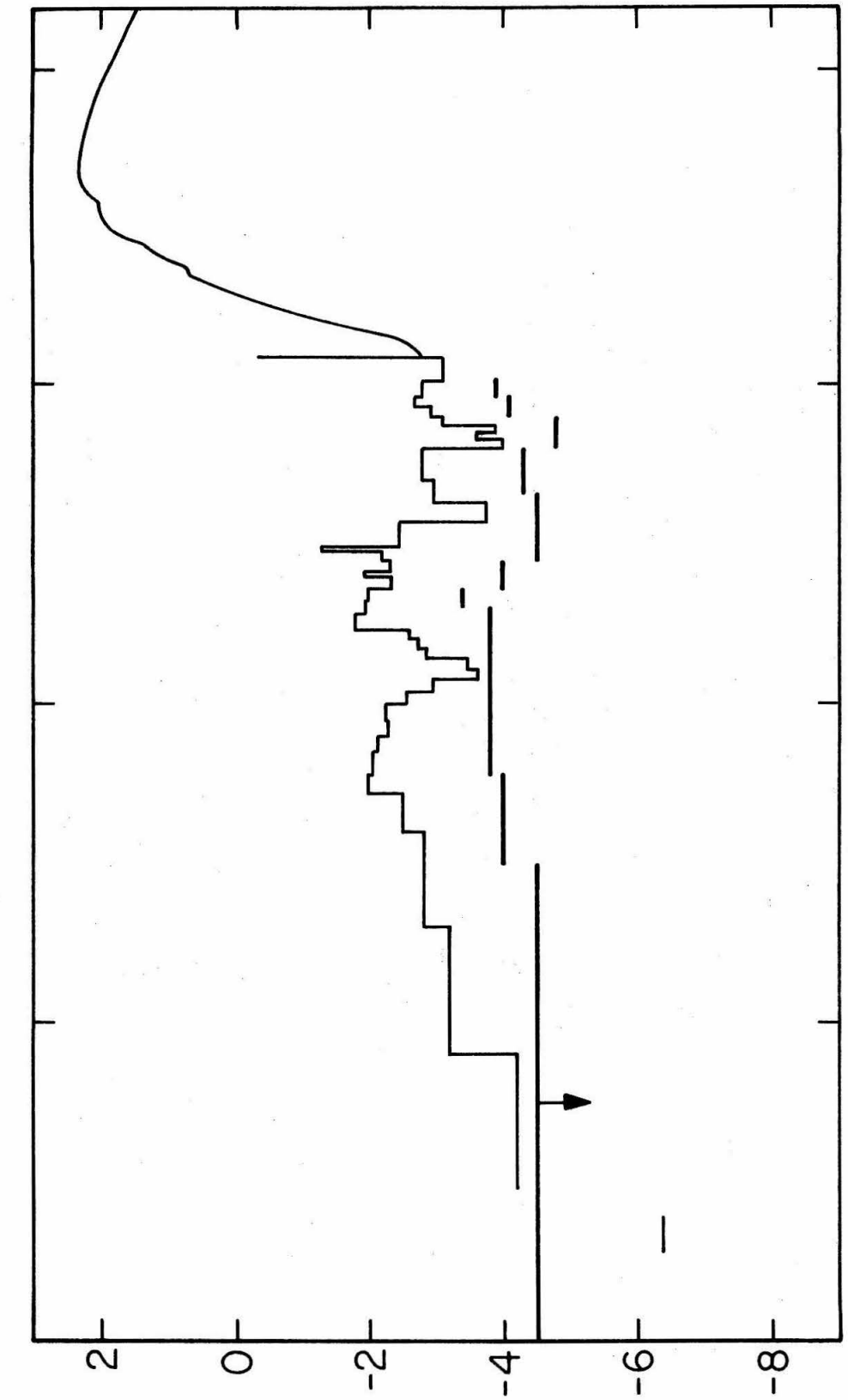

Figure 11